

# TRANSPORTATION ANALYSIS OF THE FERMILAB HIGH-BETA 650 MHz CRYOMODULE \*

J. Helsper<sup>†</sup>, S. Cheban, FNAL, Batavia, IL, USA  
I. Salehinia, Northern Illinois University, DeKalb, IL, USA

## Abstract

The prototype High-Beta 650 MHz cryomodule for the PIP-II project will be the first of its kind to be transported internationally, and the round trip from FNAL to STFC UKRI will use a combination of road and air transit. Transportation of an assembled cryomodule poses a significant technical challenge, as excitation can generate high stresses and cyclic loading. To accurately assess the behavior of the cryomodule, Finite Element Analysis (FEA) was used to analyze all major components. First, all individual components were studied. For the critical/complex components, the analysis was in fine detail. Afterwards, all models were brought to a simplified state (necessary for computational expenses), verified to have the same behavior as their detailed counterparts, and combined to form larger sub-assemblies, with the ultimate analysis including the full cryomodule. We report the criteria for acceptance and methods of analysis, and results for selected components and sub-assemblies.

## INTRODUCTION

### pHB650 Design

As designed, the prototype High-Beta 650MHz Cryomodule (pHB650 CM) contains six jacketed cavities each with their own coupler, tuner, local magnetic shield, and connection to the two-phase pipe. Hydroformed bellows are used in the beamline and cryogenic piping to provide flexibility during assembly and reduce stresses during cool down. Each cavity has two supports that are mounted to the strongback, which in turn, is connected to the vacuum vessel, as shown in Fig. 1. A 50 K thermal shield protects the cold mass from radiation, and a global magnetic shield is mounted to the inner wall of the vacuum vessel. In total, the full CM assembly is approx. 12,500 kg, 10 m long, 2 m wide, and 2 m tall. Further design details can be found in [1].

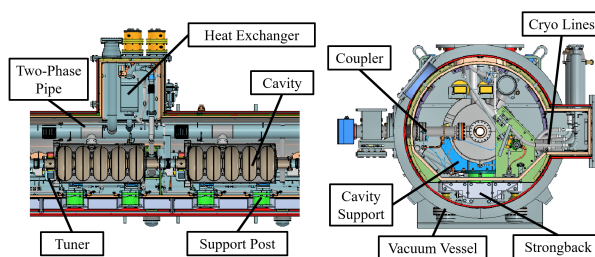


Figure 1: pHB650 CM components. Left: partial transverse section view. Right: partial axial section view.

\* Work supported by Fermi Research Alliance, LLC under Contract No. DEAC02-07CH11359 with the United States Department of Energy

<sup>†</sup> jhelsper@fnal.gov

## Transportation Scheme

The prototype HB650 CM will be built at FNAL, three production CMs will be an in-kind contribution from STFC UKRI of the U.K., and one CM kit will be provided by RRCAT of India. The trans-Atlantic transportation of the STFC UKRI CMs poses a significant risk, as previous CM transport failures have occurred which resulted in significant setbacks [2]. FNAL therefore set requirements for the transport frame and CM to mitigate these risks. The frame designed by STFC UKRI must not allow shocks greater than 3.5 G axial, 2.5 G vertical, or 1.5 G transverse on the CM, and 80% isolation must be achieved for shocks above 10 Hz. It is required that the CM components are designed to withstand 5 G axial, 3 G vertical, and 1.5 G transverse acceleration without yielding (some margin given over the frame requirements, but the transverse acceleration could not be increased due to design constraints), and critical components are to be designed to have frequencies above 20 Hz to mitigate fatigue failure.

To validate the CM design, cold RF and transportation testing will be performed separately onsite at FNAL, and afterwards, the prototype CM will be shipped to the U.K. and back via road/air transit. Prior to this shipment, a shipment of a dummy CM will take place to the U.K. to validate the transport configuration and logistics. The transport frame utilizes wire-rope isolators to mitigate shocks to the CM. The transport configuration with top port removed is shown in Fig. 2.

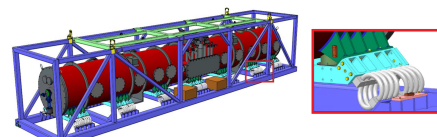


Figure 2: pHB650 CM in transport configuration within the transport frame.

## ANALYSIS AND MODELING METHODS

### Analysis Methods

ANSYS® Mechanical™ R19 was used to perform the Finite Element Analysis (FEA). While in reality road excitation comes as momentary shocks, Static Structural linear-elastic analysis was used to study the cases of 5 G axial, 3 G vertical, and 1.5 G transverse since applying the maximum acceleration as a static load should yield conservative estimates of stress and deflection. Modal analysis was used to determine the resonant frequencies of each system. Dynamic structural and harmonic analyses were considered for structural

and vibration analysis, respectively, but were rejected due to the need for accurate damping factors which can only be obtained experimentally, in addition to high computational expense compared to static structural and modal analyses.

Due to its complexity, a highly systematic approach was necessary to analyze the CM, which is summarized in Fig. 3.

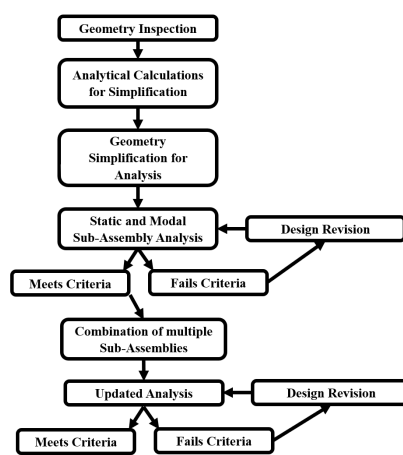


Figure 3: High-Level overview of analysis methodology.

First, individual components and sub-assemblies were analyzed in relatively high detail. Analytical calculations were performed as necessary for components not suitable for FEA (fasteners and bellows typically). Component interfaces were given high attention as they can exhibit complex behavior which is difficult to characterize in FEA. Boundary conditions (B.C.'s) approximated the component's expected loads from the larger assembly. Since these B.C.'s can induce artificial stiffness in the system, the target minimum natural frequency was set as 30 Hz so that the 20 Hz requirement could be met. While only required for critical components (bellows and beamline components), it was deemed best practice to avoid low resonant frequencies for all CM components. The structural analysis criteria was that stresses must always be below yield. If either structural or modal criteria were not met, the design was improved, however, some exceptions were made if it seemed reasonable the component would meet the requirements in further analysis. In all cases, if previous analysis had been performed (for example in an FNAL engineering note), the results were checked to match.

Afterwards came simplification of the geometry and mesh, which was necessary for computational expenses. All simplified models were verified to affect the next larger sub-assembly in the same manner, and either had a similar stress/frequency response as their detailed counterparts, or had a measurable response that could be correlated to the original response.

Last came successive model combination to form larger sub-assemblies, and ultimately the full CM assembly, as shown in Fig. 4. With each addition came renewed analysis, B.C.'s, and connections which more accurately represented the true system. As necessary, design revisions were made. It should be noted that a few sub-assemblies were left out

of the final model as their behavior was not going to change and their presence would have had negligible affects on the assembly results (see Fig. 4).

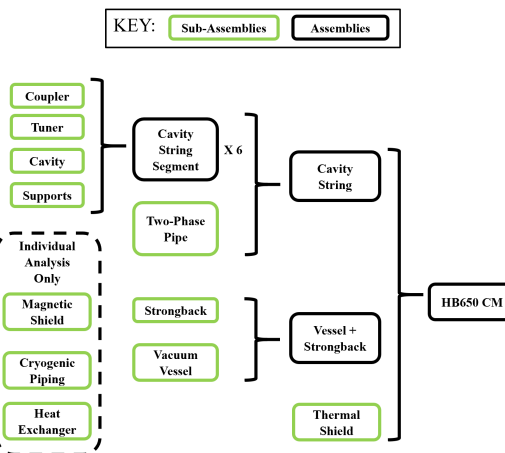


Figure 4: Analysis and combination scheme of components.

### Modeling Methods and Bellows

Nearly all geometry used for analysis was created natively in ANSYS® DesignModeler. While initially labor intensive, this approach had considerable time savings due to direct geometry editing and improved meshing quality. Shell and swept solid mesh were used primarily to reduce computational expenses, and all elements were quadratic. All contacts were linear to be compatible with the modal analysis, which proved challenging as it limited the available contact methods. Generally, multiple contact formulations were tested to evaluate the most/least conservative behavior possible, and from that best engineering practices were used to determine a path forward.

While often simplified using bushing elements, the hydro-formed bellows geometries were maintained for this analysis. By finely controlling each bellow mesh, each bellow had less than 1,000 elements. A comparison of the analytically predicted spring rates and those computed in FEA showed strong agreement, however the stresses were generally much higher in FEA. Due to the incorrect stress behavior, analytical calculations were performed to verify the fatigue life of each bellow was acceptable, with the input being the maximum displacements recorded. The minimum acceptable cycles was conservatively estimated at 220,320. This was done by assuming that a bellow had one maximum deflection every minute, each followed by 50 cycles of oscillation before damping, and the active transport lasting 3 days, yielding 220,320 cycles.

## ANALYSIS AND RESULTS

A brief overview of B.C.'s, results, design improvements, and topics of interest will be given for each sub-assembly and assembly.

## Sub-Assemblies

**Coupler** The coupler was fixed at the flange connecting to the cavity, and point masses accounted for attached components. The highest stress of 31 MPa was at the antenna due to 5 G and the first mode was 37 Hz for the antenna. A simplified model defeatured the location of highest stress, and replaced the antenna with beam elements. While this lead to inaccurate stresses, the stress could be inferred by the antenna deflection, which had a linear correlation with stress in the original model. The simplified model had 5,500 nodes, compared to 266,000 for the detailed model, and both meshes are shown in Fig. 5.

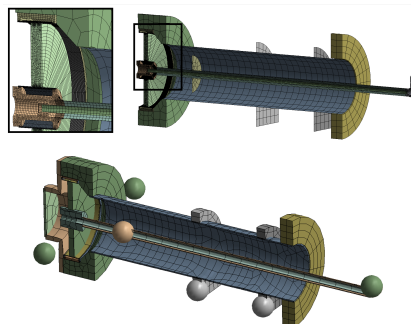


Figure 5: Section views of detailed (top) and simplified (bottom) coupler models.

**Tuner** The pads which attach to the cavity were fixed, and revolute joints were included for the bearings. The analysis showed no issues for either stress or modal behavior, with a first mode of 80 Hz, and a maximum stress of 90 MPa. Simplification was performed to reduce the number of elements and eliminate complex contacts while retaining the mass distribution, as shown in Fig. 6. This did increase the stiffness of the tuner (+35% first mode), but was confirmed to not affect any results of the cavity string segment assembly.

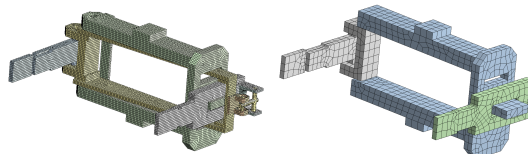


Figure 6: Tuner models.

**Accelerating Cavities** The pHB650 CM will have three beta 0.90 (B90) and three beta 0.92 (B92) cavities, but due to their similarity only the B90 will be discussed. The lugs which attach to the cavity supports were given fixed constraints, and axial springs were added to mimic the tuner stiffness. The first mode was 73 Hz transverse as shown in Fig. 7 and all stresses were well below yield. These results agreed strongly with FNAL engineering note for the cavity [3]. As the model only contained 35,000 nodes, there was no need for simplification.

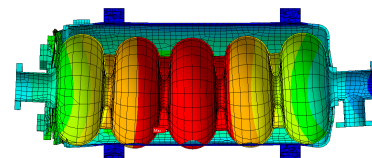


Figure 7: B90 cavity transverse mode shape.

**Cavity Supports** The lower face of each support which bolts the strongback was fixed. Each set of supports carries approx. 270 kg, which was simulated using a dummy cavity and point mass. This weight is borne by the adjustable needle block assemblies shown in Fig. 8. The behavior of the needle blocks is complex due to the numerous rotating frictional ‘push-only’ contacts. Axially and vertically, the lug is well constrained, but the transverse direction only has one contact, and so it is possible to see movement during a 1.5 G transverse acceleration, as shown in Fig. 9.

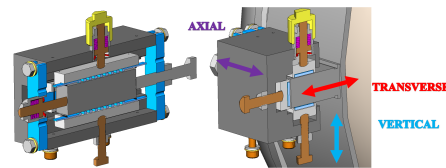


Figure 8: Needle blocks.



Figure 9: Cavity transverse movement.

Analytical calculations found the friction force insufficient to prevent transverse movement. If the cavity were to shift position during a shock, and not fully return, the string alignment could be compromised. This case was conservatively estimated with analytical methods, which found the maximum friction force that could hold open a gap between the needle block and cavity lug. This force was then applied as a separating force to determine the affect on the cavity position.

Structural and modal analysis of the support did not highlight any issues. Due to the high importance of these alignment results, the separation analysis was performed using the more complete cavity string segment model.

**Two-Phase Pipe and Heat Exchanger** The two-phase pipe model was fixed at the tee connection to each cavity, and the model is shown in Fig. 10. Invar rods run the length of the pipe, and are only fixed at the far ends to prevent excess forces on the bellows due to internal pressure. The contact between the rod’s guides and the rod allowed for rotation, but not vertical or transverse movement.

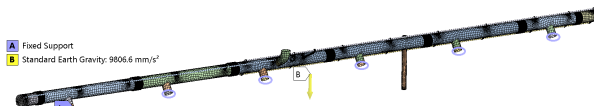


Figure 10: Two-phase pipe model.

The end sections of the two-phase pipe were found to be too flexible, which caused for excessive bellows deformation, and a 13 Hz resonant mode, which is shown in Fig. 11. The solution was to lessen the mass of the pipe past the bellows, and add additional Invar rod guides to constrain the motion. Additionally, a 10 Hz mode for the helium level sensor (contained in the vertical pipe shown on the right side of Fig. 10) was improved by adding an internal support.

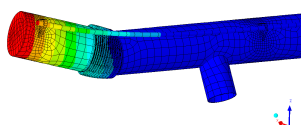


Figure 11: Two-phase pipe 13 Hz mode shape.

As the heat exchanger is not installed for overseas shipment, it was analyzed separately and was not included in the full CM analysis. The model used only the adjoining segments of the two-phase pipe (refer to Fig. 1 for location). The cantilevered heat exchanger design led to low resonant frequencies and excessive stress at the base weld, and so a low thermal conductivity support was added to resolve this.

**Cryogenic Piping** The 2 K line, 5 K line, pumping relief line, relief valve, and cryogenic valves were all checked. The only issue found was a low frequency axial mode in the 5 K line, which was resolved by adding unidirectional supports to both ends. All except the pumping relief line were left out of the final model.

**Thermal and Magnetic Shields** The thermal shield is mounted to each support post, but only axially fixed at the center post to allow for thermal contraction. Due to 5 G, the shield and attached components created a significant shearing load, and so the center post bolts attaching the shield were enlarged. A connecting plate to the vessel, along with G10 studs that thread through the shield and contact the vessel, were added for stability to improve low resonant modes.

The global magnetic shield is mounted directly to the inner wall of the vacuum vessel, and is well supported. The end plates experienced low frequency resonance / yielding due to 5 G axial loading, and this was resolved by adding a simple L-Channel across the end plate. The local magnetic shielding for each cavity saw no issues. The global shielding was not included in the final model as it was deemed unlikely to affect other components' response.

**Strongback and Supports** The strongback was fixed at its 14 connection points to the supports, and was given a

4,000 kg point mass to simulate the cold mass. Both modal and structural results were acceptable and agreed with those of CEA (of France) who designed the strongback [4]. The first mode was 32 Hz rocking transversely, and the model is shown in Fig. 12.

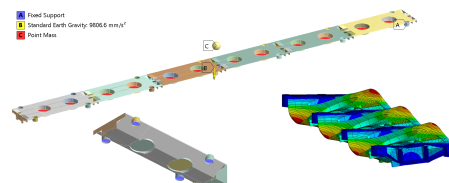


Figure 12: Strongback model and 1st mode shape.

The strongback support model included a portion of the vessel to decrease artificial rigidity, forces for loads and cold mass weight, and restricted rotation on the top plate to mimic the strongback stiffness. Stresses and modes were acceptable, although analytical calculations showed the need for increased fastener sizes due to the shearing load. Both the detailed and simplified models exhibited near identical behavior, and are shown in Fig. 13.

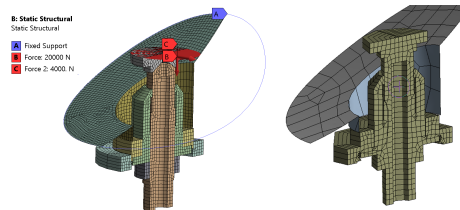


Figure 13: Section views of detailed (left) and simplified (right) strongback support models.

**Vacuum Vessel** The vacuum vessel model was fixed at the transport mounts, and a point mass accounted for the cold mass weight. No issues were found in modal or structural analyses. The lowest mode was 38 Hz transverse and the highest stresses were at the transport mounts due to 5 G.

### Assemblies

**Cavity String Segment** The cavity string segment consisted of the following, which is shown in Fig. 14: B90/B92 cavity, tuner, coupler, two cavity supports, and a point mass for the two-phase pipe. Compared to the model with cavity supports and dummy cavity, this model saw a slightly lower transverse resonant frequency, caused by the offset center of gravity due to the heavy tuner.

By applying 600 N of force to create the misalignment scenario previously explained, the cavity moved transversely by 0.41 mm, and to maintain alignment, they must move <0.25 mm. Therefore, the support was redesigned to be much stiffer, which resulted in a maximum movement of 0.19 mm. After this, the needle blocks were greatly simplified due to their many nodes and contacts. Approximating the needle block as a fixed connection was too stiff in the axial direction, causing deflection to decrease by 45%. Allowing the joint

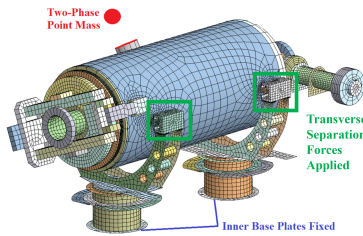


Figure 14: Cavity segment model.

to rotate proved not stiff enough, instead overshooting the original axial deformation by 31%. The solution was to add a torsional spring which approximated the rotational stiffness of the needle block, and this led to the results matching within 5% for nearly all structural and modal results. The mode shape and simplified needle block are shown in Fig. 15.

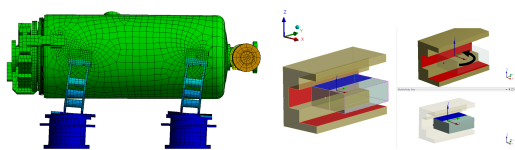


Figure 15: Left: contour plot of axial deformation. Right: torsion spring around x-axis.

**Cavity String** The cavity string model consisted of six string segments, their interconnecting bellows, and the two-phase pipe. Modal analysis found no issues, but the two-phase pipe modes were significantly lower than before due to the lack of artificial rigidity. What was previously a 34 Hz mode dropped to 23 Hz. Structural analysis largely matched results from sub-assemblies, but the two-phase pipe's decreased stiffness caused for an increased deflection on one bellows, which an additional Invar rod guide was able to mitigate to achieve the desired life cycle rating. The transverse mode of the string was 21 Hz, only 1 Hz lower than the cavity segment.

**Vessel and Strongback** The vessel, strongback, and strongback supports were combined into a single model, and point masses accounted for the cold mass and global magnetic shield weights. Structural analysis showed good agreement with previous work with some expected differences. The vessel saw slightly higher stresses due to the mass from the magnetic shield, and the strongback supports saw less stress due to decreased rigidity. Modal analysis found that, as expected, the strongback transverse mode dropped significantly, from 32 Hz to 23 Hz.

**Full Cryomodule** The full CM model contained the cavity string, thermal shield, strongback, and vacuum vessel, as shown in Fig. 16. In total, the model contained 601,000 nodes, 178,000 elements, and the first 50 modes were solved in 30 minutes with high-performance PC.

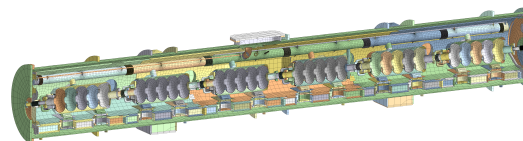


Figure 16: Full cryomodule model

The first mode saw the transverse rocking of the cold mass at 18 Hz, 3 Hz lower than for the string. While below 20 Hz, this was not of concern due to the low likelihood for high amplitude oscillation, and the fact that the deflections from this analysis showed all bellows met their life cycle requirements. Structural analysis found no significant differences from previous analysis, with all stresses allowable.

Further information on methods and results can be found at the following sources [5], [6].

## CONCLUSION

The pHB650 CM was analyzed for vibration and directional shock loading in preparation for its overseas shipment. Several aspects of the design were improved, and CM design was validated as ready for transportation. The methods utilized in this work give a clear path to future cryomodule engineers seeking to perform analysis on complex systems, and help to illustrate the need for detailed analysis, accurate B.C.'s, and proper model optimization.

## ACKNOWLEDGEMENTS

The work completed could not have been accomplished without support from J. Holzbauer, V. Roger, S. Chandrasekaran, G. Wu, Y. M. Orlov, N. Tanovic, G. Smith, N. Pohlman, and S. Butail.

## REFERENCES

- [1] V. Roger *et al.*, "Design of the 650 MHz high beta prototype cryomodule for PIP-II at Fermilab," presented at SRF'21, Grand Rapids, Michigan, USA, Jun. 2021, paper WEPTEV015.
- [2] N. Huque *et al.*, "Improvements to LCLS-II cryomodule transportation," in *Proc. SRF '19*, Dresden, Germany, Jun. 2019, paper TUP094, pp. 686-691. doi:10.18429/JACoW-SRF2019-TUP094
- [3] N. Nigam *et al.*, "PIP-II 650 MHz  $\beta=0.9$  jacketed cavity engineering analysis report ED0010266," unpublished, 2019.
- [4] M. Lacroix, "Strongback - Mechanical," presented at PIP-II 650 MHz High Beta Prototype Cryomodule Final Design Review, 2020. <https://indico.fnal.gov/event/43274/>
- [5] J. Helsper, "Transportation analysis and related design optimization of the Fermilab high-beta 650 MHz cryomodule," M.S. thesis, College of Eng. and Eng. Tech., North. Ill. Univ., DeKalb, 2020. <https://www.osti.gov/biblio/1764073>
- [6] S. Cheban and J. Helsper, "Transportation analysis," presented at PIP-II 650 MHz High Beta Prototype Cryomodule Final Design Review, 2020. <https://indico.fnal.gov/event/43274/>